# Behaviour and Fate of Anthropogenic Gadolinium in Groundwater

## Insights from Batch Experiments and Measured Concentrations in the Besòs River Delta (NE Spain)

Pujades-Garnes, Estanislao; Ekiz, Mert Çetin; Izquierdo, Maria; Scheiber, Laura; Salehi Siavashani, Nafiseh; Jurado, Anna; Vázquez-Suñé, Enric; Foppen, Jan Willem

**DOI**
10.1007/s40710-025-00784-0

**Publication date**
2025

**Document Version**
Final published version

**Published in**
Environmental Processes

**Citation (APA)**
Pujades-Garnes, E., Ekiz, M. Ç., Izquierdo, M., Scheiber, L., Salehi Siavashani, N., Jurado, A., Vázquez-Suñé, E., & Foppen, J. W. (2025). Behaviour and Fate of Anthropogenic Gadolinium in Groundwater: Insights from Batch Experiments and Measured Concentrations in the Besòs River Delta (NE Spain). *Environmental Processes*, *12*(3), Article 43. https://doi.org/10.1007/s40710-025-00784-0

Environmental Processes (2025) 12:43
https://doi.org/10.1007/s40710-025-00784-0

RESEARCH

# Behaviour and Fate of Anthropogenic Gadolinium in Groundwater: Insights from Batch Experiments and Measured Concentrations in the Besòs River Delta (NE Spain)

**Estanislao Pujades-Garnes[1] · Mert Çetin Ekiz[2] · Maria Izquierdo[1] · Laura Scheiber[1] · Nafiseh Salehi Siavashani[1] · Anna Jurado[1] · Enric Vázquez-Suñé[1] · Jan Willem Foppen[3]**

Received: 14 February 2025 / Accepted: 19 June 2025

## Abstract

Urban aquifers are a potential alternative, with which to cover the rising demand for freshwater. However, they are commonly polluted by a wide range of anthropogenic substances, including rare earth elements (REEs). In this context, it is essential to investigate the presence and behaviour of these pollutants, in order to safely use urban groundwater. An example of these contaminants is Gadolinium, which can reach the environment after it has been used for medical purposes. Gadolinium anomalies were detected in hydraulically connected surface and subsurface water bodies in Barcelona, northeast Spain. A striking factor in this study, is that Gadolinium pollution in groundwater was less frequent and more attenuated than in surface water, suggesting that Gadolinium attenuation may be prevalent in the subsurface. Batch experiments were conducted and modelled to ascertain processes affecting Gadolinium in the sampled aquifers. Experimental results have (i) demonstrated that the concentration of dissolved Gadolinium decreased 90% in 24 days, and (ii) suggested that sorption plays a key role in Gadolinium attenuation. The modelling of the experiments provides essential parameters, with which to predict the behaviour of Gadolinium. Our results have significant implications for understanding the evolution of anthropogenic Gadolinium in aquifers in general, which is of paramount importance for determining where groundwater can be safely used after its natural or artificial infiltration.

## Highlights

- Anthropogenic gadolinium ($Gd_{ANT}$) has been detected in urban water bodies.
- The distribution of $Gd_{ANT}$ suggests that its concentration decreases in aquifers.
- Batch experiments are developed and modelled to ascertain processes affecting $Gd_{ANT}$.
- Experiments reveal that sorption may affect the concentration of $Gd_{ANT}$ in aquifers.

**Keywords** Gadolinium-based contrast agents · Urban aquifer · Hydrochemical modelling · Batch experiment · Sorption

---

Extended author information available on the last page of the article

## 1 Introduction

Different pressures impacting on water resources are increasing dramatically, and also in urban areas, as a result of climate change and growing demand for safe drinking water. Therefore, it is necessary to consider new sources of freshwater, such as urban groundwater bodies. However, such bodies are commonly polluted by urban anthropogenic contaminants, such as contaminants of emerging concern (CECs), that compromise the usefulness of urban groundwater (Richardson and Kimura 2017), and reach aquifers from multiple sources (i.e., leakage from sewers, effluents from wastewater treatment plants, industrial site pollution) (Vázquez-Suñé et al. 2010; Nikolenko et al. 2023). Considering that physicochemical and mechanical processes occurring in aquifers can contribute to mitigate the concentration of some CECs, it is of paramount importance to characterize these processes, in order to establish when and where urban groundwater can be safely used.

The Rare Earth Element (REE) Gadolinium (Gd) is considered to be a contaminant of emerging concern (CEC) that has been detected in urban aquifers (Brünjes and Hofmann 2020a). Although Gd occurs naturally, it can also originate from discharges from industrial and/or urban areas. For example, Gd is used in Magnetic Resonance Imaging (MRI) applications to aid blood vessel visualization (Trapasso et al. 2021). Due to the high toxicity of the $Gd^{3+}$ free ion (Coimbra et al. 2024), Gd is used in chelated forms in Gd-Based Contrast Agents (GBCAs). GBCAs are composed of a polyaminocarboxylic acid ligand, which derives from either the linear, acyclic compound $H_5DTPA$ or the macrocyclic compound $H_4DOTA$ (Le Fur and Caravan 2019). This reduces its toxicity, as the chelated forms are hydrophilic, thermodynamically stable, and kinetically inert (Le Fur and Caravan 2019). After MRI scans, GBCAs are excreted from the body (Le Fur and Caravan 2019; Trapasso et al. 2021) and then they reach sewers, from which they can leak into aquifers or be conducted to wastewater treatment plants (WWTPs) (Trapasso et al. 2021). Later, GBCAs that are not removed in WWTPs are released into surface water bodies (rivers, creeks, or lakes), and they can infiltrate aquifers. Anthropogenic Gadolinium ($Gd_{ANT}$) has been detected in water bodies from various parts of the world since 1996 (Wang et al. 2021). It is expected that GBCA discharges will increase, due to the growing (Kulaksız and Bau 2011a; Brünjes and Hofmann 2020b) and ageing population, as older people require more medical attention, but also because of the increasing access to healthcare for all citizens in the society (Pereto et al. 2023). Moreover, after the recent coronavirus disease (COVID-19) pandemic, GBCAs have been excessively used to detect heart damage caused by SARS-CoV-2, which could contribute to increased Gd pollution (Souza et al. 2021). Although typical $Gd_{ANT}$ concentrations detected in water bodies are lower than levels that are considered to be toxic (Rogowska et al. 2018), the transformation products of these compounds, or the release of $Gd^{3+}$ ions, could potentially pose toxic risks to human health and aquatic life (Hanana et al. 2017). $Gd^{3+}$ can cause problems in the skeleton, cardiac muscles, transmission of nervous influx, and blood coagulation (Rogowska et al. 2018; Trapasso et al. 2021), and GBCAs can accumulate in tissues (e.g., bone and brain) (Fraum et al. 2017). Note that, a recent study has concluded that concentrations exceeding 100 µg/L, which are frequently observed in polluted rivers, present a moderate teratogenic risk (Cesarini et al. 2024). However, significant knowledge gaps remain regarding the environmental impact of Gd complexes, particularly concerning their effects on aquatic and terrestrial organisms, as well as their degradation, metabolization, and bioaccumulation (Rogowska et al. 2018).

$Gd_{ANT}$ in surface waters has been reported worldwide. For example, concentrations close to 0.01 µg $L^{-1}$ Gd have been documented in San Francisco Bay in the USA (Hatje et al. 2016), in the Rhine river (Germany) (Knappe et al. 2005; Bau et al. 2006; Kulaksız and Bau 2011a), or the Garonne River (France) (Lerat-Hardy et al. 2019). Higher concentrations, exceeding 0.1 µg $L^{-1}$, have also been reported downstream of industrial effluent plumes (Knappe et al. 2005; Kulaksız and Bau 2011b, 2013; Ebrahimi and Barbieri 2019). $Gd_{ANT}$ has recently even been detected in waters from fjords, and a river in southern Norway, as well as at multiple coastal stations in Denmark and Sweden (Zocher et al. 2025). The ratio between background (i.e., natural) settings and $Gd_{ANT}$ is highly site-dependent. For example, Hatje et al. (2016) reported anthropogenic concentrations that were 1.6 to 3.9 times higher than in natural settings, Knappe et al. (2005) reported anthropogenic values 1.6 to 1.8 times higher, Kulaksız and Bau (2011a) found anthropogenic values 0.95 to 644 times higher, Lerat-Hardy et al. (2019) reported anthropogenic values 1.15 to 6.83 times higher, Kulaksız and Bau (2011b) observed anthropogenic values 0.98 to 110 times higher, and Ebrahimi and Barbieri (2019) reported anthropogenic values 1.2 to 1.9 times higher.

Gd concentration in aquifers is usually lower than in surface water bodies and wastewater (Atinkpahoun et al. 2020), which could suggest that processes occurring within the aquifer or the riverbed have the potential to attenuate the concentration of $Gd_{ANT}$. Among the different processes, sorption seems to be the most important, as reported by investigations that were specifically focused on groundwater. In their study, Noack et al. (2014) concluded that the presence of oxides and clays allows for the effective removal of REEs from more neutral and basic groundwaters through sorption. Möller et al. (2011), who reported the importance of sorption in a column experiment simulating a bank filtration system, also detected that the most important process for removing $Gd_{ANT}$ is transmetalation (i.e., Gd ions in GBCAs are exchanged/replaced by other metals; Kulaksız and Bau 2011a). Tang and Johannesson (2010) observed that Carrizo Sand, which is a geological formation located primarily in Texas (USA) with significant aquifer capacity, quickly adsorbed Gd, and in general, all REEs. Similarly, Kautenburger and Beck (2010) investigated the sorption of Gd on kaolinite, at different concentrations in order to establish its isotherm, while Hamadneh et al. (2021) used diatomaceous earth (and modified diatomaceous earth) as the adsorbent. Despite the relevance of these studies, their results are very site- and material-specific.

Overall, to our knowledge, the physico-chemical processes affecting GBCAs in aquifers are not yet fully understood. Enhancing our understanding of the mechanisms controlling the fate of these gadolinium compounds is crucial for predicting their behaviour in aquifers. To address these issues, the present work seeks to (i) assess the occurrence and distribution of $Gd_{ANT}$ in surface and groundwater in an urban Mediterranean area; and (ii) shed light on the processes contributing to the attenuation of $Gd_{ANT}$ in aquifers through a laboratory batch experiment simulating groundwater environments, in conjunction with modelling work. The modelling of the experiments provides the equations and parameters that characterize the behaviour of $Gd_{ANT}$, which will be valuable for predicting its performance in different scenarios, such as managed aquifer recharge.

## 2 Materials and Methods

### 2.1 Study Area and Water Sampling

We surveyed two water bodies at the Besòs River delta (Northern Barcelona in NE Spain). From a hydrogeological perspective, the Besòs River Delta consists of two aquifers: a deep confined aquifer formed by a basal layer of coarse and medium gravels, and a shallow unconfined aquifer made up of gravels, sands, and silts, which is hydraulically connected to the Besòs River. These aquifers are separated by an aquitard composed of silts and clays. The entire formation, including both aquifers and the intermediate aquitard, is made up of Quaternary alluvial deposits that overlay, in discordance, Pliocene and Palaeozoic clays and sands (Velasco et al. 2012). Concerning the climatic conditions, the study area experiences a typical Mediterranean climate (i.e., sub-tropical) with an average annual rainfall of approximately 600 mm. Specifically, water samples from the Besòs River were collected at three locations (R1 to R3), and groundwater samples from the shallow aquifer of the Besòs River delta were collected at eight monitoring points (Aq1 to Aq8) (Fig. 1). River water was monitored during a single field campaign, undertaken in February 2021, while groundwater samples were taken at two different periods (June 2020 and February 2021) to determine the temporal variability. Four of the eight groundwater monitoring points were surveyed during the two field campaigns (Aq4, Aq5, Aq6, and Aq8 in Fig. 1). The interaction between these two water bodies depends on the location. On the upgradient side of the delta (between R2 and Aq6 in Fig. 1), the river and the aquifer are hydraulically connected, and the river receives water from the aquifer; in the middle part (between Aq6 and Aq4 in Fig. 1) the piezometric head is below the elevation of the river bed, and thus, the aquifer receives water from the river through a leakage; and in the lower part (from Aq4 towards

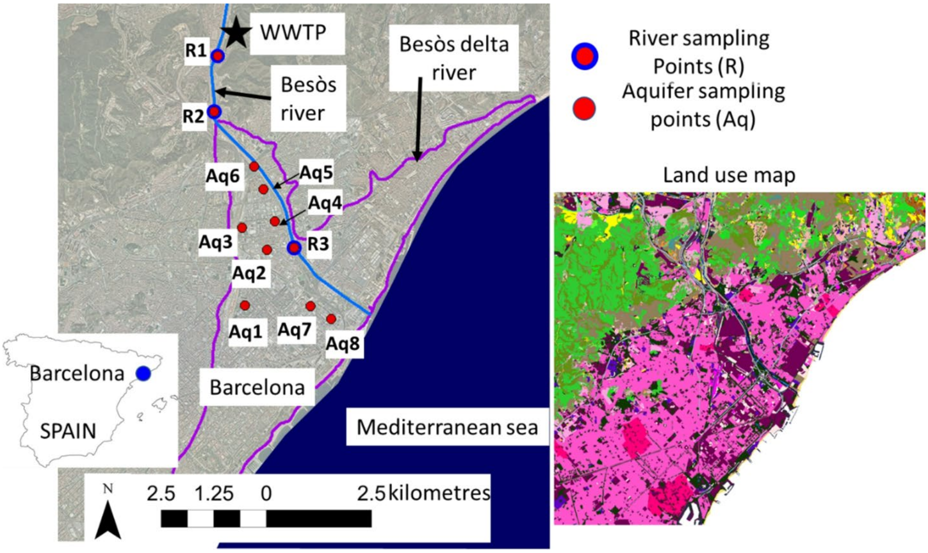

**Fig. 1** Study area and sampling locations. Red dots: aquifer points (Aq1–Aq8); red dots with blue outline: river points (R1–R3). Purple line: Besòs River delta boundary; blue line: river course; black star: wastewater treatment plant. Right panel shows land use, with pink for urban and purple for industrial areas, highlighting anthropogenic influence

the sea) the river and the aquifer are hydraulically connected and they exchange water bi-directionally, depending on the site. River samples were collected 200 m downstream of effluent discharge of a WWTP (R1), before the urbanized area located downstream of the WWTP (R2) (1500 m from the WWTP), and in the middle of the urbanized area that is also located downstream of the WWTP (R3) (5300 m from the WWTP).

Groundwater samples were taken from observation wells, after measuring the piezometric head and purging their inner water for a specific period of time to remove stagnant water. During the purging period, in-situ field parameters (redox potential, pH, dissolved oxygen, temperature, and electrical conductivity) were monitored with a Hanna multiparametric probe to ensure that samples were taken after stabilization. River water was sampled directly after measuring the in-situ field parameters. Total alkalinity (TAC) was also measured in the field by acid-base titration using an Aquamerck alkalinity kit. Water samples were collected in high-density 15 mL polyester containers.

## 2.2 Analyses of Water and Solutions

An aliquot of water was collected in a 20 ml muffled glass bottle, filtered through 0.45 μm nylon filter, acidified with 2 N HCl, and analyzed for DOC concentration by the catalytic oxidation method at 680 °C, using a Shimadzu TOC-V CSH instrument. Another aliquot was collected in a high-density 15 mL polyethylene tube, and it was used to determine the concentrations of major anions using a Thermo Scientific Dionex Aquion ion chromatography system with supressed conductivity detection. The system operates with Dionex IonPac AS9-HC 2 mm and AG9-HC 2 mm analytical and guard columns, respectively, and Dionex AERS 500 Carbonate suppressor. The limits of quantification were 3 and 10 μg $L^{-1}$ for nitrate and sulphate, respectively. A third aliquot was collected in a high-density 15 mL polyethylene tube, and it was adjusted to 1% $HNO_3$ v/v, and analyzed using a Thermo-Fisher Scientific iCAP-RQ ICP-MS instrument operating with a collision-cell using He with kinetic energy discrimination. Peak dwell times for $^{57}$Fe, $^{157}$Gd, $^{147}$Sm, and $^{159}$Tb were 0.01s, 100 quadrupole sweeps and 3 runs. Sample processing was undertaken with Thermo-Fisher Scientific Qtegra™ software, utilizing external cross-calibration between pulse-counting and analogue detector modes when required. A solution of 5 μg $L^{-1}$ In in 1% $HNO_3$ was used as the internal standard. The instrument was calibrated using synthetic solutions diluted from SPEX CertiPrep multi-elemental stock solutions in the range 0–50 μg $L^{-1}$ for Gd, Sm, and Tb and 0–1000 μg $L^{-1}$ for Fe. A TraceCERT® synthetic standard diluted from concentrated single element stock solutions and containing 25 μg $L^{-1}$ Gd, Sm, Tb, and 100 μg $L^{-1}$ Fe was inserted in the run to check analytical accuracy. The % errors i.e., percentage value of the difference between the measured and expected concentrations divided by the actual concentration, were in the range 1.1–2.3%. An acid digestion of NIST CRM 1633b, produced in-house, was used for further calibration verification. Recoveries of 97% and 109% were reported for Fe (certified value) and Gd (non-certified value), respectively. The limits of detection, calculated as three times the standard deviation of 15 analytical blank samples, were 1.4 μg $L^{-1}$ for Fe, 0.0004 μg $L^{-1}$ for Gd, 0.0006 μg $L^{-1}$ for Sm, and 0.0004 μg $L^{-1}$ for Tb.

### 2.3 Quantification of Anthropogenic *Gadolinium ($Gd_{ANT}$)*

Because ICP-MS only measured the total Gd in solution, discrimination between anthropogenic-derived and naturally occurring (geogenic) Gd ($Gd_{BCK}$) in the river and groundwater samples was attempted using mathematical approaches, while assuming a specific behaviour of Gd in relation to other individual REEs (Brünjes et al. 2016). Firstly, REE solution concentrations were normalized to the composition of a geological reference material, namely, Post Archean Australian Shale (PAAS) (McLennan et al. 1980). This normalization is needed because when the concentration of measured REEs is plotted, the resulting plot commonly shows a zigzag pattern that is caused by the Oddo-Harkins rule (Gwenzi et al. 2018; Mihajlovic and Rinklebe 2018). These zigzag patterns can be eliminated by normalizing the concentration of REEs against a standard. Once REEs are normalized, anomalies can identify and quantify the anthropogenic portion of specific REEs. We used the PAAS standard to normalize the measured REEs, because (i) no significant differences were observed when using PAAS or other reference materials, such as the North American Shale Composite, and (ii) PAAS is widely used in research. When REEs are normalized according to standards and plotted, sharp increases can be observed in specific REEs in the case of pollution (Merschel et al. 2015). To avoid overestimation of $Gd_{ANT}$, a threshold value of 1.1 was selected to identify anomalies, and to differentiate between anthropogenic and natural Gd (Wang et al. 2021). $Gd_{BCK}$ concentrations were calculated by comparing them with neighbouring REEs (Brünjes et al. 2016). Europium (Eu) and Cerium (Ce) were dismissed because of the existence of naturally occurring anomalies in both contaminated (Kulaksız and Bau 2011b; Zhu et al. 2016; Wang et al. 2021) and uncontaminated water bodies (Shahhosseini et al. 2017). Thus, interpolation was undertaken based on the measured concentrations of Sm and Tb (Table 1), which were shale-normalized, as suggested by Shiller (2002), Bau et al. (2006), and Brünjes et al. (2016) (Eq. 1).

**Table 1** Measured Gd concentrations ($Gd_{TOTAL}$) at the sampling points, along with calculated anthropogenic ($Gd_{ANT}$) and natural background ($Gd_{BCK}$) values. Sm and Tb concentrations are also reported, as they are used to estimate Gd background levels

| Site | $Gd_{TOTAL}$ (ng $L^{-1}$) | $Gd_{BCK}$ (ng $L^{-1}$) | $Gd_{ANT}$ (ng $L^{-1}$) | Sm (ng $L^{-1}$) | Tb (ng $L^{-1}$) |
|---|---|---|---|---|---|
| River | | | | | |
| R1 | 173.0 | 1.1 | 171.9 | 0.5 | 0.2 |
| R2 | 167.0 | 1.7 | 165.3 | 1.9 | 0.3 |
| R3 | 133.0 | 1.7 | 131.3 | 1.7 | 0.3 |
| Aquifer (1st field campaign – 2020) | | | | | |
| Aq1 | 4.9 | 6.3 | 0.0 | 5.3 | 1.2 |
| Aq2 | 4.3 | 4.9 | 0.0 | 5.2 | 0.9 |
| Aq3 | 26.2 | 5.3 | 20.9 | 4.0 | 1.0 |
| Aq4 | 23.5 | 1.7 | 21.8 | 1.9 | 0.3 |
| Aq5 | 56.4 | 6.1 | 50.3 | 4.4 | 1.2 |
| Aq6 | 61.5 | 8.2 | 53.3 | 5.6 | 1.6 |
| Aq7 | 12.6 | 10.3 | 2.3 | 6.2 | 2.1 |
| Aq8 | 16.0 | 4.8 | 11.2 | 3.3 | 1.0 |
| Aquifer (2st field campaign – 2021) | | | | | |
| Aq4 | 34.2 | 4.9 | 29.3 | 0.5 | 1.2 |
| Aq5 | 71.5 | 8.0 | 63.4 | 3.6 | 1.7 |
| Aq6 | 65.5 | 6.5 | 59.0 | 3.6 | 1.3 |
| Aq8 | 11.3 | 2.6 | 8.7 | 0.5 | 0.6 |

$$Gd_{BCK} = (0.33 * Sm_n + 0.67 * Tb_n) * Gd_{PAAS} \tag{1}$$

where $Gd_{BCK}$ is the background concentration of Gadolinium, $Sm_n$ is the normalized concentration of Samarium, $Tb_n$ is the normalized concentration of Terbium, and $Gd_{PAAS}$ is the concentration of Gadolinium in the PAAS standard. The anthropogenic component of Gd ($Gd_{ANT}$) was then computed by subtracting the estimated $Gd_{BCK}$ from the total measured Gd.

## 2.4 Experimental Setup

### 2.4.1 Hydrochemical Conditions – Field Data Vs. Simulated Conditions

The chemical conditions for conducting the experiment were chosen considering the general hydrochemistry of the delta aquifer. In general, the groundwater of the aquifer ranges from low-aerobic to anaerobic conditions, based on dissolved oxygen (DO) measurements, taken during the two sampling campaigns, and on previous studies conducted in the Besòs delta aquifers ((Jurado et al. 2020; Sáez et al. 2024). DO concentrations during the field campaigns ranged from 1.3 to 3 mg/L (average of 2.2 mg/L). These conditions can also be inferred from the comparison between nitrate concentrations in the aquifer and in the river during the sampling campaigns. Excluding two points where the concentration was very high (over 70 mg/L), likely influenced by leaks from sewers, nitrate concentrations in the aquifer ranged from 11.4 to 26.4 mg/L (average of 17.3 mg/L) during the first campaign, and from 3.4 to 22.2 mg/L (average of 10 mg/L) during the second campaign. In contrast, nitrate concentrations in the river were higher than those of the aquifer, ranging between 37.8 and 80.1 mg/L (average of 63.7 mg/L), which might indicate that nitrate was reduced under nitrate-reducing redox conditions.

### 2.4.2 Experimental Design

The experiment consisted of three reactors, each containing 796 g of sediment collected from the riverbed of the Besòs River, to mimic similar conditions of the study area. The collected sediment was air dried in darkness, and sieved to <2 mm to ensure homogeneity between the reactors. To each reactor, 2150 mL of a mixture of 80% synthetic water and 20% water collected from Besòs Delta river aquifer water were added (Fig. 2). Synthetic water composition, in accordance with the work of Bolster et al. (1999), allowed (i) minimizing the concentration of contaminants from the aquifer that facilitated interpretation and modelling, and (ii) ensured the homogenization between reactors, while aquifer water acted as inoculum. Note that a sediment-water ratio close to 1:2.5 was selected, based on the previous works, with the aim of mimicking the conditions of Barcelona's aquifers (Nödler et al. 2012; Barbieri et al. 2012). A larger ratio was not considered, in order to avoid zoning within the sediment with different redox conditions, while a smaller ratio was not chosen, in order to prevent minimizing the surface area that was available for sorption processes to occur. A fourth 'control' reactor with no sediment was also included (Fig. 2). The objective of this control reactor was to determine whether the presence of the soil contributed to the removal of Gd through sorption processes. After 7 days acclimatization at room temperature, the 4 reactors were spiked with a freshly made solution of gadodiamide ($C_{16}H_{26}GdN_5O_8$; CAS

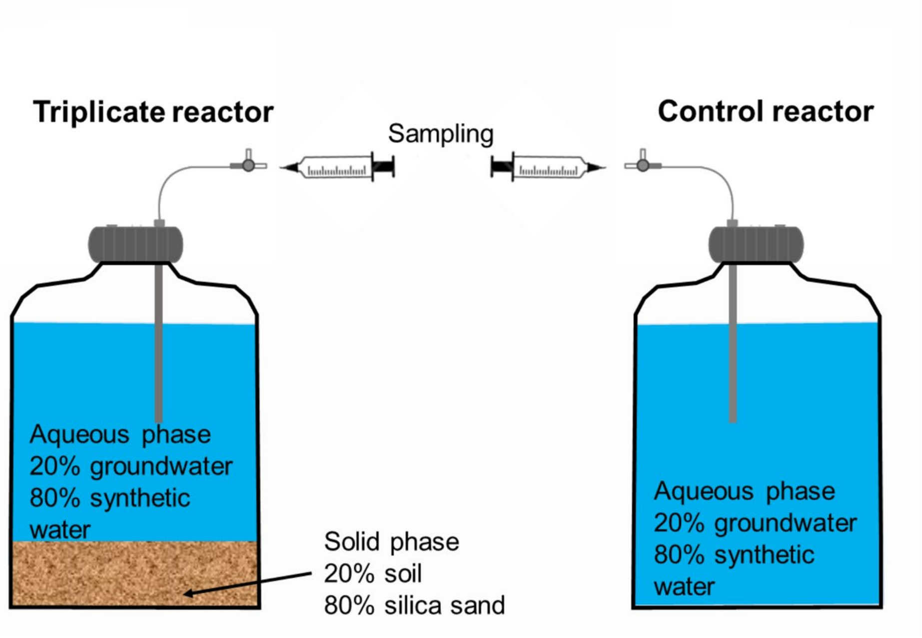

**Fig. 2** Schematic view of the design of the triplicate (left) and the control reactors used in the experiment

no.131410-48-5) to provide a final aqueous concentration of 250 mg $L^{-1}$ (≈66 mg $L^{-1}$ of Gadolinium). We focused on Gadodiamide because, although other Gd species may be more stable, they are likely to be less environmentally relevant as anthropogenic sources of Gd. Gadodiamide is one of the most widely used GBCAs, and there is strong evidence that this particular compound is released into the environment after being excreted from the body, and then discharged into wastewater systems. The added concentration was intentionally set higher than levels observed in the field, in order to: (i) prevent misinterpretation due to naturally occurring gadolinium in the water or soil used in the experiment, (ii) reduce the sample volume required for analysis, thereby minimizing variation in the solid-to-liquid ratio within each bottle, and (iii) decrease the influence of analytical errors on the results.

To promote bacterial growth, biodegradable dissolved organic matter (BDOC) was added to the reactors at the beginning of the experiment, to give a final concentration of 10 mg $L^{-1}$. This consisted of a 6:4 (wt/wt) mixture of Merck lactate (high BDOC) and Merck humic acid (low BDOC), to reproduce aquifer conditions of the sampled site. The sampled aquifer present sub-oxic to anoxic conditions which can only occur if high BDOC (like lactate) is available. For this reason, the proportion of lactate was higher than humic acid. Two BDOC sources were combined to promote microbial diversity (Regnery et al. 2015). pH ranged from 7.75 at the beginning to 7.50 at the end of the experiment. The reactor extracts were analyzed as described in Sect. 2.2.

### 2.4.3 Sampling and Analysis

The reactors were incubated for 10 days at 20 ° C, and in darkness to avoid photochemical degradation due to UV light and algae growth (Trapasso et al. 2021). Incubation and sampling were conducted inside a glove box filled with $N_2$ to maintain anoxic conditions throughout the experiment. After 1, 2, 3, 6, 8, and 10 days following contamination, an aliquot of 40 mL was removed from each reactor to determine the concentrations of anions, Gd, Fe, and DOC in solution. An additional sample was taken after 21 days, in order to determine the final Gd and Fe concentrations in the reactors.

## 2.5 Numerical Modelling

Laboratory experiments were modelled using the PHREEQC code (Parkhurst 1995; Parkhurst and Appelo 1999; Parkhurst et al. 2010), and calibrated automatically with PEST (Doherty 1994). PHREEQC is code that solves speciation problems, batch-reaction processes, one-dimensional transport, and inverse geochemical calculations, while PEST is code for developing non-linear parameter estimation that can be combined with multiple simulation codes, and it is based on the Gauss-Marquardt-Levenberg method (Doherty 1994).

# 3 Results and Discussions

## 3.1 Field Data

Table 1 shows the measured Gd concentrations ($Gd_{TOTAL}$) in the sampling sites, and estimated anthropogenic ($Gd_{ANT}$) and geogenic Gd ($Gd_{BCK}$) concentrations for the samples taken at the river and at the groundwater monitoring points in the two sampling campaigns. The precision of Gd measurements in terms of %RSD were in the range 1.4–3.6%. The concentration of Sm and Tb are included in Table 1 since they are used to calculate the background concentration of Gadolinium using Eq. 1. The spatial distribution of estimated $Gd_{ANT}$ concentrations using data from the two sampling campaigns is shown in Fig. 3. River concentrations are included in both figures (Fig. 3a and b).

**River Samples** $Gd_{ANT}$ was detected in all river samples, with the highest concentration reported at R1. This Gd anomaly likely reflects treated wastewater inputs, given the vicinity of a major WWTP, located 200 m upstream, that is processing most of the wastewater of the metropolitan area of Barcelona. The concentration of $Gd_{ANT}$ reduces downstream, suggesting that physico-chemical processes occur in the river-bed. Analyzing riverbed sediments could provide deeper insight into the processes influencing Gd concentrations at the river-aquifer interface. The effect of a possible dilution as a result of groundwater inflows is assumed to be marginal, since inflows would promote an abrupt decrease in the concentration of Gd in the river. In addition, some samples were taken at locations (near sampling site R3) where it is well-known that river water infiltrates in the aquifer as a result of adjacent pumpings (Sáez et al. 2024). Note that, river samples were collected only once and were not integrated, since the use of autosamplers was not possible due to logistical and safety

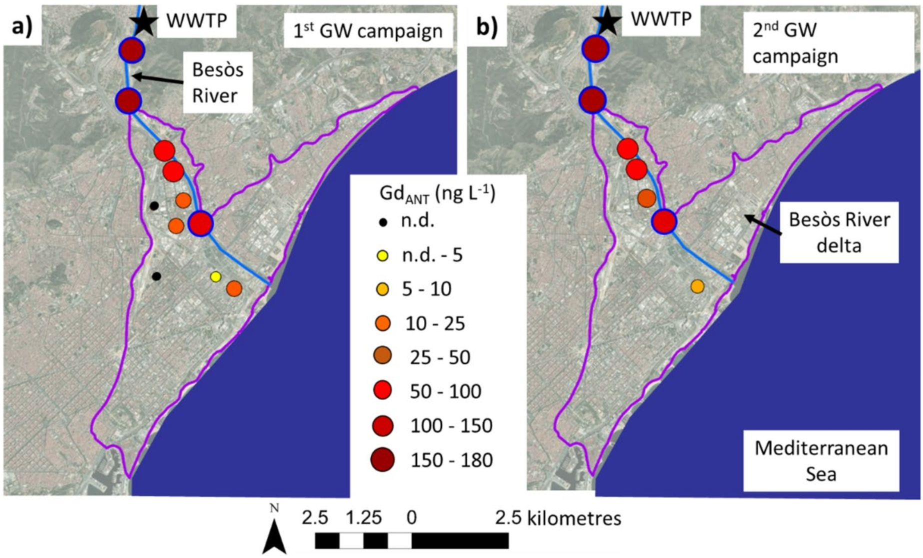

**Fig. 3** Observed $Gd_{ANT}$ concentrations from the first (Fig. **3a**, left) and second (Fig. **3b**, right) sampling campaigns. Points with blue outlines: river samples; others: aquifer. Purple line: delta boundary; blue line: river; black star: WWTP location

reasons. However, we do not expect the main conclusions of this paper to be affected by this limitation.

The concentration of $Gd_{ANT}$ in the river indicates pollution, with levels comparable to those reported in rivers in Germany (Kulaksız and Bau 2011b), where concentrations have reached up to 190 ng/L, or in the USA (Smith and Liu 2018), where reported concentrations reached 256 ng/L. Our observations in the present study confirm that WWTP effluents have the potential to increase $Gd_{ANT}$ concentrations in river water, as noted by other authors (Klaver et al. 2014; Merschel et al. 2015). In particular, $Gd_{ANT}$ concentrations 200 m downstream of the WWTP effluent discharge were greater than those reported in WWTPs from South Korea (Song et al. 2017), Australia (Lawrence et al. 2009), or the USA (Verplanck et al. 2005), and lower than what was reported by Knappe et al. (2005) in Germany, although WWTP effluent discharges may substantially vary throughout the week, typically peaking by Friday (Brünjes et al. 2016). The decrease in $Gd_{ANT}$ downstream is also in line with the results of other studies (Wang et al. 2021) and reflects attenuation processes affecting GBCAs, including direct sunlight photodegradation (Trapasso et al. 2021) and adsorption onto riverbed sediments. Water exchanges between river and aquifer may further reduce $Gd_{ANT}$ levels in the river, as a result of dilution processes and/or GBCAs infiltration into the aquifer (Atinkpahoun et al. 2020; Wang et al. 2021).

**Groundwater Samples** Despite the fact that $Gd_{ANT}$ was detected in most groundwater samples (at 75% of the sampled locations), its concentration is, at least, 1-fold lower than in the river (Table 1). Considering that our previous studies found that the Besòs River is hydraulically well connected with the shallow deltaic aquifer (Jurado et al. 2021; Nikolenko et al.

2024), and confirms a bi-directional exchange between these two water bodies, the comparison between measured $Gd_{ANT}$ in the river and in the aquifer suggests that $Gd_{ANT}$ concentration was attenuated in the aquifer. To shed light on the mechanisms and transformations that Gd may undergo at the river-aquifer interface, and in groundwater, we conducted a batch experiment. Regarding the temporal variability of gadolinium, the comparison of concentrations at the four sampled points during the two field campaigns suggests that it is low, as the largest difference is 13.09 ng/L. This fact seems to indicate that inputs into the aquifer from the river, or from other sources (e.g., sewer leaks), are relatively constant over time.

Numerous studies have been conducted in the investigated aquifer focusing on water quality; however, this is the first study centered on the presence of gadolinium. Therefore, we are unable to compare our findings with previous studies from the same research area. Most of the research carried out in recent years has focused on the occurrence and behavior of emerging organic contaminants such as pharmaceutical compounds, personal care products, or PFAS. Among others, Jurado et al. (2021) investigated the presence and behavior of non-steroidal anti-inflammatory drugs and evaluated their attenuation potential under suboxic to denitrifying conditions. Saéz et al. (2024) studied the occurrence and behavior of PFAS, identifying key processes—such as redox-driven attenuation, sorption/desorption, and transformation—that govern their evolution along the groundwater flow. Bautista et al. (2024) identified up to 148 polar and highly polar organic compounds in a study conducted in the Besòs River delta aquifer. These studies suggest that the Besòs River delta aquifer has the capacity to attenuate the concentrations of a wide range of organic contaminants. In comparison with investigations conducted in other aquifers, the concentration of $Gd_{ANT}$ in the Besòs delta aquifer was lower than that reported by other authors in groundwater bodies from the USA (Johannesson et al. 2017) or Germany (Knappe et al. 2005). Johannesson et al. (2017) investigated the behavior of REEs in subterranean estuaries along the Kona Coast of Hawaii (USA), highlighting the key role of groundwater as a major source of dissolved REEs to coastal waters via submarine groundwater discharge. Knappe et al. (2005) investigated the occurrence and persistence of $Gd_{ANT}$ in groundwater systems of Berlin (Germany) highlighting its utility as a conservative tracer for identifying and quantifying the infiltration of recycled surface water into aquifers.

## 3.2 Laboratory Experiment

### 3.2.1 Hydrochemical Evolution

**Major Ions, Oxygen and DOC** Figure 4a shows the evolution of dissolved oxygen (DO), nitrate ( $NO_3^-$), and iron ($Fe^{2+}$) during the experiment. The concentration in the reactors has been averaged since error bars are not observed, because the plot is semilogarithmic. The low initial DO levels indicate that the experiment started with poorly aerobic conditions, as most DO was consumed during the acclimatization phase. Addition of synthetic BDOC, real groundwater (20%), and sediment from the river bed as inoculums, introduced bacteria into the reactors and prompted microbially-mediated redox changes, rapidly reaching suboxic/denitrifying conditions where $NO_3^-$ was consumed. This was followed by reductive dissolution of insoluble $Fe^{3+}$ releasing $Fe^{2+}$ into solution, reaching Fe reducing conditions after 6 days.

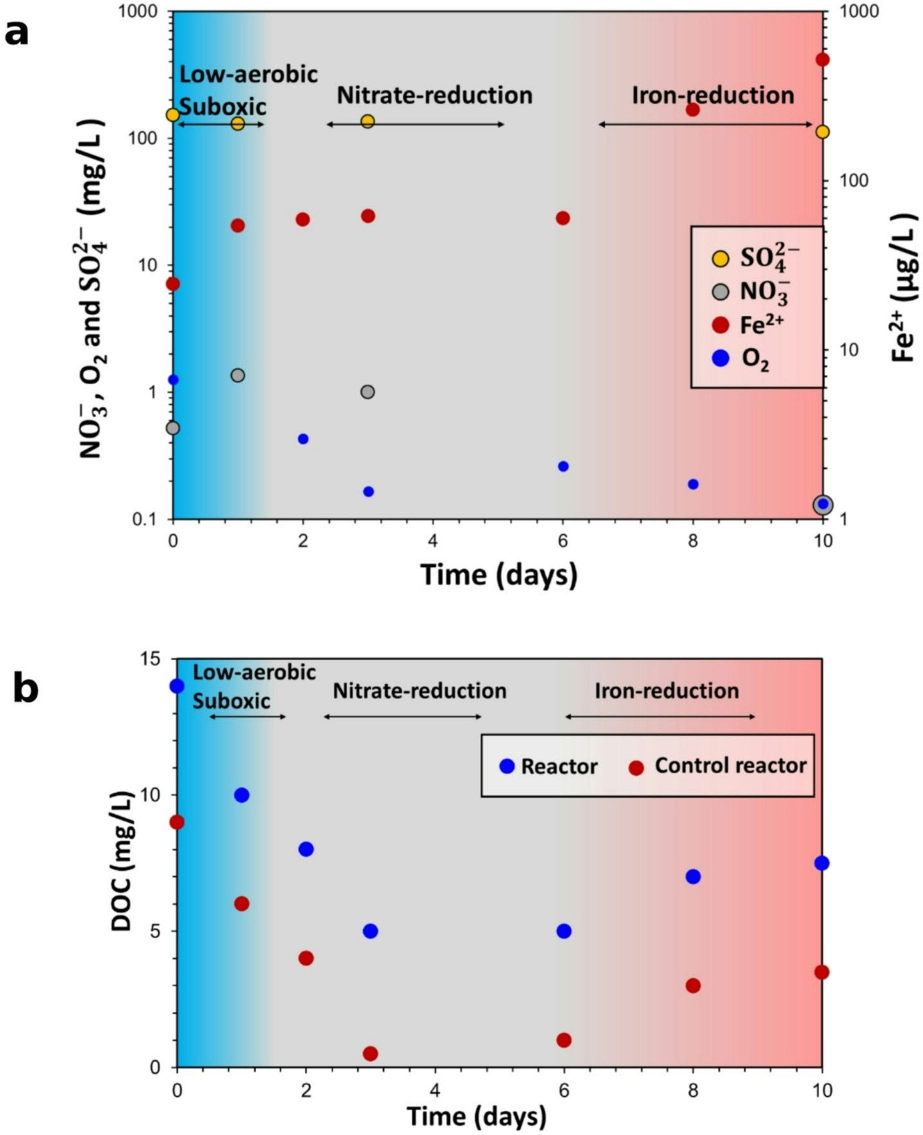

**Fig. 4** (**a**) Evolution of dissolved DO, $NO_3^-$, $Fe^{2+}$, and $SO_4^{2-}$ during the experiment. (**b**) BDOC evolution in experimental and control reactors. Background shading indicates redox state changes

The concentration of DOC in the experimental reactors (Fig. 4b) was higher than in the control reactor, and about 10 ppm greater than what was initially added as synthetic BDOC at the beginning of the experiment, reflecting the addition of organic matter-rich riverbed sediments to the reactors. DOC concentrations decreased during the nitrate-reducing phase, and started to increase after day 6. According to Laufer et al. (2016), DOC can increase during the reduction of $Fe^{3+}$.

Figure 5 shows the correlation matrix considering major ions, DO, and DOC in the triplicate reactors to deduce their relationship. The highest correlation is observed between DOC and DO, which is expected since organic matter (i.e., DOC) is initially degraded in the presence of DO. Therefore, both DOC and $O_2$ decreased during the first part of the experiment. The correlation between DOC and $SO_4^{2-}$ is moderately high, which is due to both species decreasing throughout the experiment. What is noteworthy, is the low correlation between DOC and $NO_3^-$, as a high correlation was expected. The low correlation may be related to the fact that DOC decreases in the presence of oxygen, and increases during the iron reduction phase, while $NO_3^-$ remains constant during both stages. DO also shows a moderate correlation with $SO_4^{2-}$, because both decrease during most of the experiment. The correlation between $NO_3^-$ and DO is low, which could be explained by the fact that $NO_3^-$ remains constant during the initial decrease of DO. Finally, $Fe^{2+}$ correlates negatively with $SO_4^{2-}$ and $NO_3^-$, as both decrease while $Fe^{2+}$ increases during the iron reduction phase.

**Gd Evolution** According to the body of literature, GBCAs may undergo dechelation or transmetallation reactions (Runge 2018), thereby releasing free $Gd^{3+}$. Transmetallation rates and extent vary among GBCAs, depending on the molecular structure (Sherry et al. 2009), the presence of competing ions (Elizalde-González et al. 2017), or environmental binding partners, such as humic acid (Sommer et al. 2022). Our analyses did not allow differentiating between the different forms of Gd, and only provided the total concentration of dissolved Gd in water. Therefore, we cannot determine whether the measured Gd is in the form of Gadodiamide or free Gd ions. Thus, hereinafter, we shall refer to total Gd. Figure 6 shows the time-dependent removal of total Gd from solution in relation to the initial concentration of Gd spiked in gadodiamide form. Total Gd steadily decreased in the experimental reactors, whilst largely remaining stable in the control reactor. The comparison between the evolution of Gd concentration in the experimental reactors and in the control reactor (without soil, but with the same water and organic matter) indicates that sediment plays a key role in the attenuation of Gd in gadodiamide forms through sorption processes. These observations agree with the previous literature, where sorption is recognized as a key process in the elimination of Gd from water in different water matrices (Kautenburger and Beck 2010; Noack et al. 2014; Johannesson et al. 2017; Liu et al. 2017; Hamadneh et al. 2021; Mohamed et al. 2022; Cendón et al. 2022). In our experiment, the sorption capacity of the sediments reached up to 0.15 mg of Gd/gram of sediment. The marginal decrease reported for the control reactor could be associated with adsorption of gadodiamide onto colloidal organic matter, which is in agreeance with previous works that identify organic matter as an adsorbent of REES (Kautenburger 2009; Davranche et al. 2015). In addition, the decrease of Gd in the control reactor occurs after day 5, which is when the concentration of DOC increased (increasing

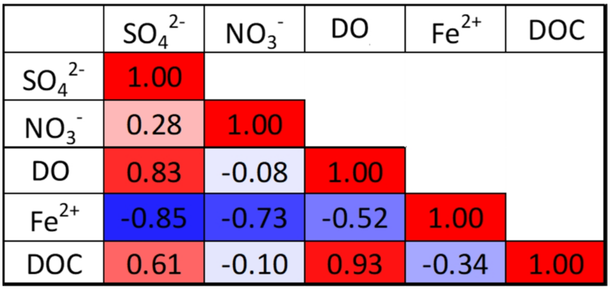

**Fig. 5** Correlation matrix between major ions $NO_3^-$, $Fe^{2+}$, $SO_4^{2-}$, DO and DOC, during the experiment with the three reactors

| | $SO_4^{2-}$ | $NO_3^-$ | DO | $Fe^{2+}$ | DOC |
|---|---|---|---|---|---|
| $SO_4^{2-}$ | 1.00 | | | | |
| $NO_3^-$ | 0.28 | 1.00 | | | |
| DO | 0.83 | -0.08 | 1.00 | | |
| $Fe^{2+}$ | -0.85 | -0.73 | -0.52 | 1.00 | |
| DOC | 0.61 | -0.10 | 0.93 | -0.34 | 1.00 |

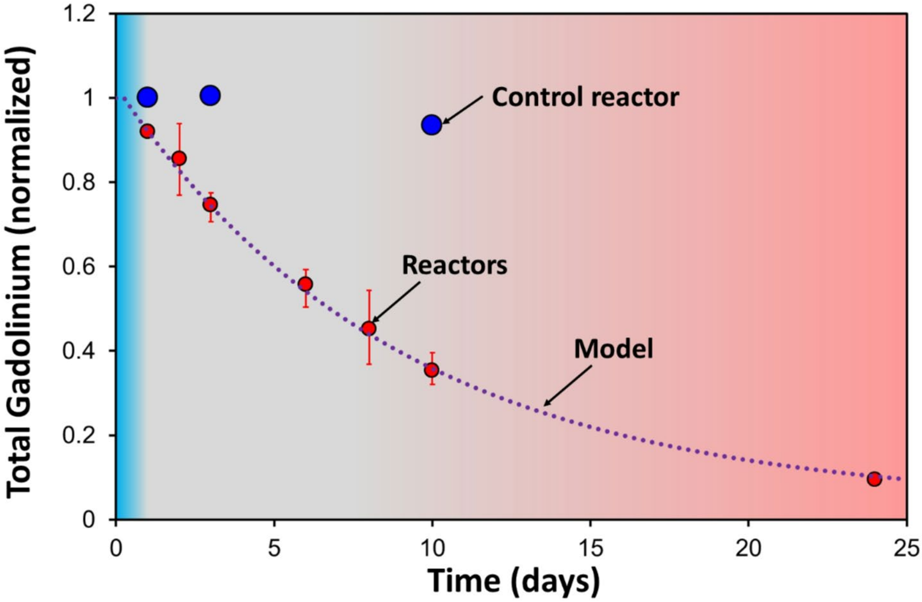

**Fig. 6** Normalized Gd concentrations over time in experimental reactors (red dots), control reactor (blue dot), and modelled values (purple line). Background shading indicates redox state changes

also the amount of potential adsorbent), as a result of the iron reduction phase. Finally, it is noteworthy that, according to the Gd behaviour and redox conditions throughout the experiment, the Gd sorption rates do not seem to be redox-sensitive.

### 3.2.2 Modelling

Time-dependent reductions in Gd concentrations in solution were modelled, assuming that sorption is the main process that controls its attenuation. Total Gd removal was found to conform to the Valocchi sorption reaction rate model (Zhang et al. 2012) (Eq. 2).

$$R_k = -k_m \left(C - S/k_d\right) \tag{2}$$

where $R_k$ is the sorption rate, $C$ is the concentration of the aqueous-species (mol/L), $S$ is the adsorbed concentration, $k_m$ is a mass-transfer coefficient, and $k_d$ is the distribution coefficient. $k_m$ and $k_d$ were calibrated by using PEST and the resulting values were 3.53E-6 $s^{-1}$ and 0.56 L/g, respectively. The model fittings are shown in Fig. 6. Goodness of fit was assessed by calculating the correlation coefficient (0.99) and the Residual Standard Deviation (0.95). Contrary to previous works, where Gd sorption has been modelled assuming isotherm models, such as the Langmuir or Freundlich models (Kautenburger and Beck 2010; Liu et al. 2017), in the present work, the sorption of Gd is modelled using a sorption kinetics model. While adsorption isotherms are relevant to explain the interaction between Gd and an adsorbent (in this case the aquifer matrix) and the optimum adsorption capacity of the adsorbent, adsorption kinetics allows simulating the rate at which the Gd is adsorbed. Note that, the evolution of the redox sequence was also modelled with PHREEQC, using

Monod equations with inhibition factors, that were needed to prevent the activation of more advanced stages of the redox sequence, as long as the previous acceptor compound was still present. However, these numerical results are not included in this paper since, as deduced from Figs. 4 and 6, the redox state does not affect gadolinium attenuation.

## 4 Conclusions

Gd anomalies were detected in the Besòs River (Barcelona) and in the hydraulically-connected aquifer of the Besòs delta (maximum detected concentrations of $Gd_{ANT}$ were 172 and 63 ng $L^{-1}$ in the river and the aquifer, respectively). These anomalies could be partially attributed to WWTP discharges upstream, supporting the hypothesis that Gd from medical sources is a major contributor to anomalous Gd loadings in surface water bodies (i.e., the maximum concentration of $Gd_{ANT}$ was detected at the location of the WWTP, and decreased downstream). However, additional samples should be collected upstream of the WWTP, in order to confirm that the plant is the main source of anthropogenic Gd.

Field observations suggest that $Gd_{ANT}$ is attenuated in the subsurface, according to the levels of Gd measured in the aquifer and the river. The average concentration of $Gd_{ANT}$ in the river was 156 ng $L^{-1}$, while its average concentration in the aquifer was 20 and 40 ng $L^{-1}$ during the first and second field campaigns, respectively.

Experimental results revealed that sorption seems to be the main process involved in the attenuation of $Gd_{ANT}$. The sorption is rapid and non-redox-sensitive (at least until Fe reduction conditions), as the concentration of dissolved gadolinium decreased by 90% over the 24-day period of the experiment. Experimental results are consistent with the field observations and allow establishing that sorption is responsible for the differences in the concentration of $Gd_{ANT}$ between the river and the aquifer.

The provided kinetics of Gd sorption, which were obtained from the model, may prove useful to predict the behaviour of $Gd_{ANT}$ in aquifers when water is infiltrated (naturally or artificially). According to our results, aquifers have the capacity to improve freshwater quality by attenuating the concentration of $Gd_{ANT}$, highlighting the usefulness of managed aquifer recharge techniques to improve the quality of water. In the case of river bank filtration systems, the distance between the river and the pumping facility should be sufficient to attenuate the concentration of anthropogenic Gd by sorption. Conventional groundwater recharge using water from rivers or WWTP may also further remove anthropogenic Gd, by forcing water to flow through the aquifer.

Our analysis did not allow us to differentiate between the various forms of Gd, thus providing only the total concentration of dissolved Gd in the water. As a result, we could not determine whether the measured gadolinium is in the form of Gadodiamide or free Gd ions. Future studies should employ advanced analytical methods to distinguish aqueous species, which could enhance our understanding of the factors driving GBCA adsorption kinetics.

**Author Contributions** Estanislao Pujades-Garnes: Conceptualization, Methodology, Investigation, Writing - Original Draft, Supervision, Funding acquisition. Mert Çetin Ekiz: Conceptualization, Methodology, Formal analysis, Investigation, Writing - Review & Editing. Maria Izquierdo: Conceptualization, Investigation, Resources, Writing - Review & Editing, Supervision, Funding acquisition. Laura Scheiber: Resources, Writing - Review & Editing. Nafiseh Salehi Siavashani: Writing - Review & Editing. Anna Jurado: Conceptualization, Methodology, Writing - Review & Editing. Enric Vázquez-Suñé: Resources, Writing - Review & Editing, Funding acquisition. Jan Willem Foppen: Conceptualization, Methodology, Supervision.

**Funding** Open Access funding provided thanks to the CRUE-CSIC agreement with Springer Nature. The experimental work of this research was mostly supported by MCIU/AEI/https://doi.org/10.13039/501100011033 and FEDER "one way to make Europe" through the grant PID2021-128995OA-I00. In addition, the authors have been supported by the grants CEX2018-000794-S funded by MCIU/AEI/https://doi.org/10.13039/501100011033 and 2021-SGR-00308 funded by Generalitat de Catalunya. Individually, EP acknowledges the support from MICIU/AEI/https://doi.org/10.13039/501100011033 and European Union NextGenerationEU/PRTR through the grant CNS2023-144051 and MICIU/AEI /https://doi.org/10.13039/501100011033 and European Union through the grant PCI2024-153452. LS gratefully acknowledges the support received by Award for Scientific Research into Urban Challenges in the City of Barcelona 2020 (21S04651, 21S04652 and 21S04653) from the Barcelona city council and the European project PCI2019-103616 (URBANWAT).

**Data Availability** No datasets were generated or analysed during the current study.

## Declarations

**Competing Interests** The authors declare no competing interests.

## References

Atinkpahoun CNH, Pons M-N, Louis P et al (2020) Rare Earth elements (REE) in the urban wastewater of Cotonou (Benin, West Africa). Chemosphere 251:126398. https://doi.org/10.1016/j.chemosphere.2020.126398

Barbieri M, Carrera J, Ayora C et al (2012) Formation of diclofenac and sulfamethoxazole reversible transformation products in aquifer material under denitrifying conditions: batch experiments. Sci Total Environ 426:256–263. https://doi.org/10.1016/j.scitotenv.2012.02.058

Bau M, Knappe A, Dulski P (2006) Anthropogenic gadolinium as a micropollutant in river waters in Pennsylvania and in lake erie, Northeastern united States. Geochemistry 66:143–152. https://doi.org/10.1016/j.chemer.2006.01.002

Bautista A, Björnsdotter M, Sáez C et al (2024) Determination of persistent and mobile organic compounds in the river–groundwater interface of the Besòs river delta, spain, using a wide extraction approach. Chemosphere 368:143673. https://doi.org/10.1016/j.chemosphere.2024.143673

Bolster CH, Mills AL, Hornberger GM, Herman JS (1999) Spatial distribution of deposited bacteria following miscible displacement experiments in intact cores. Water Resour Res 35:1797–1807. https://doi.org/10.1029/1999WR900031

Brünjes R, Hofmann T (2020a) Anthropogenic gadolinium in freshwater and drinking water systems. Water Res 182:115966. https://doi.org/10.1016/j.watres.2020.115966

Brünjes R, Hofmann T (2020b) Anthropogenic gadolinium in freshwater and drinking water systems. Water Res 182:115966. https://doi.org/10.1016/j.watres.2020.115966

Brünjes R, Bichler A, Hoehn P et al (2016) Anthropogenic gadolinium as a transient tracer for investigating river bank filtration. Sci Total Environ 571:1432–1440. https://doi.org/10.1016/j.scitotenv.2016.06.105

Cendón DI, Rowling B, Hughes CE et al (2022) Rare Earth elements and yttrium as tracers of waste/rock-groundwater interactions. Sci Total Environ 830:154706. https://doi.org/10.1016/j.scitotenv.2022.154706

Cesarini G, Spani F, Patricelli R et al (2024) Assessing teratogenic risks of gadolinium in freshwater environments: implications for environmental health. Ecotoxicol Environ Saf 278:116442. https://doi.org/10.1016/j.ecoenv.2024.116442

Coimbra S, Rocha S, Sousa NR et al (2024) Toxicity mechanisms of gadolinium and gadolinium-Based contrast Agents—A review. Int J Mol Sci 25:4071. https://doi.org/10.3390/ijms25074071

Davranche M, Gruau G, Dia A et al (2015) Biogeochemical factors affecting rare Earth element distribution in shallow wetland groundwater. Aquat Geochem 21:197–215. https://doi.org/10.1007/s10498-014-9247-6

Doherty J (1994) PEST: A Unique Computer Program for Model-independent Parameter Optimisation. In: Water Down Under 94: Groundwater/Surface Hydrology Common Interest Papers; Preprints of Papers. pp 551–554

Ebrahimi P, Barbieri M (2019) Gadolinium as an emerging microcontaminant in water resources: threats and opportunities. Geosciences 9:93. https://doi.org/10.3390/geosciences9020093

Elizalde-González MP, García-Díaz E, González-Perea M, Mattusch J (2017) Removal of gadolinium-based contrast agents: adsorption on activated carbon. Environ Sci Pollut Res 24:8164–8175. https://doi.org/10.1007/s11356-017-8491-x

Fraum TJ, Ludwig DR, Bashir MR, Fowler KJ (2017) Gadolinium-based contrast agents: A comprehensive risk assessment. J Magn Reson Imaging 46:338–353. https://doi.org/10.1002/jmri.25625

Gwenzi W, Mangori L, Danha C et al (2018) Sources, behaviour, and environmental and human health risks of high-technology rare earth elements as emerging contaminants. Sci Total Environ 636:299–313. https://doi.org/10.1016/j.scitotenv.2018.04.235

Hamadneh I, Al-Jundub NW, Al-Bshaish AA, Al-Dujiali AH (2021) Adsorption of lanthanum (III), samarium (III), europium (III) and gadolinium (III) on Raw and modified diatomaceous earth: equilibrium, kinetic and thermodynamic study. Desalination Water Treat 215:119–135. https://doi.org/10.5004/dwt.2021.26762

Hanana H, Turcotte P, André C et al (2017) Comparative study of the effects of gadolinium chloride and gadolinium – based magnetic resonance imaging contrast agent on freshwater mussel, *Dreissena polymorpha*. Chemosphere 181:197–207. https://doi.org/10.1016/j.chemosphere.2017.04.073

Hatje V, Bruland KW, Flegal AR (2016) Increases in anthropogenic gadolinium anomalies and rare Earth element concentrations in San Francisco Bay over a 20 year record. Environ Sci Technol 50:4159–4168. https://doi.org/10.1021/acs.est.5b04322

Johannesson KH, Palmore CD, Fackrell J et al (2017) Rare Earth element behavior during groundwater–seawater mixing along the Kona Coast of Hawaii. Geochim Cosmochim Acta 198:229–258. https://doi.org/10.1016/j.gca.2016.11.009

Jurado A, Margareto A, Pujades E et al (2020) Fate and risk assessment of sulfonamides and metabolites in urban groundwater. Environ Pollut 267:115480. https://doi.org/10.1016/j.envpol.2020.115480

Jurado A, Vázquez-Suñé E, Pujades E (2021) Urban groundwater contamination by Non-Steroidal Anti-Inflammatory drugs. Water 13:720. https://doi.org/10.3390/w13050720

Kautenburger R (2009) Influence of metal concentration and the presence of competing cations on europium and gadolinium speciation with humic acid analysed by CE-ICP-MS. J Anal Spectrom 24:934–938. https://doi.org/10.1039/B904107A

Kautenburger R, Beck HP (2010) Influence of geochemical parameters on the sorption and desorption behaviour of europium and gadolinium onto kaolinite. J Environ Monit 12:1295–1301. https://doi.org/10.1039/B914861B

Klaver G, Verheul M, Bakker I et al (2014) Anthropogenic rare Earth element in rivers: gadolinium and lanthanum. Partitioning between the dissolved and particulate phases in the rhine river and Spatial propagation through the rhine-Meuse Delta (the Netherlands). Appl Geochem 47:186–197. https://doi.org/10.1016/j.apgeochem.2014.05.020

Knappe A, Möller P, Dulski P, Pekdeger A (2005) Positive gadolinium anomaly in surface water and ground water of the urban area Berlin. Ger Geochem 65:167–189. https://doi.org/10.1016/j.chemer.2004.08.004

Kulaksız S, Bau M (2011a) Anthropogenic gadolinium as a microcontaminant in tap water used as drinking water in urban areas and megacities. Appl Geochem 26:1877–1885. https://doi.org/10.1016/j.apgeochem.2011.06.011

Kulaksız S, Bau M (2011b) Rare Earth elements in the rhine river, germany: first case of anthropogenic lanthanum as a dissolved microcontaminant in the hydrosphere. Environ Int 37:973–979. https://doi.org/10.1016/j.envint.2011.02.018

Kulaksız S, Bau M (2013) Anthropogenic dissolved and colloid/nanoparticle-bound samarium, lanthanum and gadolinium in the rhine river and the impending destruction of the natural rare Earth element distribution in rivers. Earth Planet Sci Lett 362:43–50. https://doi.org/10.1016/j.epsl.2012.11.033

Laufer K, Byrne JM, Glombitza C et al (2016) Anaerobic microbial Fe (II) oxidation and Fe (III) reduction in coastal marine sediments controlled by organic carbon content. Environ Microbiol 18:3159–3174. https://doi.org/10.1111/1462-2920.13387

Lawrence MG, Ort C, Keller J (2009) Detection of anthropogenic gadolinium in treated wastewater in South East queensland, Australia. Water Res 43:3534–3540. https://doi.org/10.1016/j.watres.2009.04.033

Le Fur M, Caravan P (2019) The biological fate of gadolinium-based MRI contrast agents: a call to action for bioinorganic chemists. Metallomics 11:240–254. https://doi.org/10.1039/c8mt00302e

Lerat-Hardy A, Coynel A, Dutruch L et al (2019) Rare Earth element fluxes over 15 years into a major European estuary (Garonne-Gironde, SW France): Hospital effluents as a source of increasing gadolinium anomalies. Sci Total Environ 656:409–420. https://doi.org/10.1016/j.scitotenv.2018.11.343

Liu H, Pourret O, Guo H, Bonhoure J (2017) Rare Earth elements sorption to iron oxyhydroxide: model development and application to groundwater. Appl Geochem 87:158–166. https://doi.org/10.1016/j.apgeochem.2017.10.020

McLennan SM, Nance WB, Taylor SR (1980) Rare Earth element-thorium correlations in sedimentary rocks, and the composition of the continental crust. Geochim Cosmochim Acta 44:1833–1839. https://doi.org/10.1016/0016-7037(80)90232-X

Merschel G, Bau M, Baldewein L et al (2015) Tracing and tracking wastewater-derived substances in freshwater lakes and reservoirs: anthropogenic gadolinium and Geogenic REEs in lake paranoá, Brasilia. CR Geosci 347:284–293. https://doi.org/10.1016/j.crte.2015.01.004

Mihajlovic J, Rinklebe J (2018) Rare earth elements in German soils - A review. Chemosphere 205:514–523. https://doi.org/10.1016/j.chemosphere.2018.04.059

Mohamed WR, Sami NM, Metwally SS, Saad EA (2022) Surface modification of ball clay minerals with gamma irradiation polymerization for removal of cerium and gadolinium ions from aqueous phase. Hydrometallurgy 208:105816. https://doi.org/10.1016/j.hydromet.2022.105816

Möller P, Knappe A, Dulski P, Pekdeger A (2011) Behavior of Gd-DTPA in simulated bank filtration. Appl Geochem 26:140–149. https://doi.org/10.1016/j.apgeochem.2010.11.011

Nikolenko O, Pujades E, Teixidó M et al (2023) Contaminants of emerging concern in the urban aquifers of barcelona: do they hamper the use of groundwater? Chemosphere 341:140023. https://doi.org/10.1016/j.chemosphere.2023.140023

Nikolenko O, Labad F, Pujades E et al (2024) Combination of multivariate data analysis and mixing modelling to assess tracer potential of contaminants of emerging concern in aquifers. Environ Pollut 341:123020. https://doi.org/10.1016/j.envpol.2023.123020

Noack CW, Dzombak DA, Karamalidis AK (2014) Rare Earth element distributions and trends in natural waters with a focus on groundwater. Environ Sci Technol 48:4317–4326. https://doi.org/10.1021/es4053895

Nödler K, Licha T, Barbieri M, Pérez S (2012) Evidence for the microbially mediated abiotic formation of reversible and non-reversible sulfamethoxazole transformation products during denitrification. Water Res 46:2131–2139. https://doi.org/10.1016/j.watres.2012.01.028

Parkhurst DL (1995) User's quide to PHREEQE—a computer program for speciation, reaction-path, advective transport, and inverse geochemical calculations. US Geological Survey WatereResources graphical user interface for the geochemical computer program Investigations Report

Parkhurst DL, Appelo CAJ (1999) User's guide to PHREEQC (Version 2): A computer program for speciation, batch-reaction, one-dimensional transport, and inverse geochemical calculations

Parkhurst DL, Kipp KL, Charlton SR (2010) PHAST Version 2—A Program for Simulating Groundwater Flow, Solute Transport, and Multicomponent Geochemical Reactions: U.S. Geological Survey Techniques and Methods 6–A35

Pereto C, Lerat-Hardy A, Baudrimont M, Coynel A (2023) European fluxes of medical gadolinium to the ocean: A model based on healthcare databases. Environ Int 173:107868. https://doi.org/10.1016/j.envint.2023.107868

Regnery J, Wing AD, Alidina M, Drewes JE (2015) Biotransformation of trace organic chemicals during groundwater recharge: how useful are first-order rate constants? J Contam Hydrol 179:65–75. https://doi.org/10.1016/j.jconhyd.2015.05.008

Richardson SD, Kimura SY (2017) Emerging environmental contaminants: challenges facing our next generation and potential engineering solutions. Environ Technol Innov 8:40–56. https://doi.org/10.1016/j.eti.2017.04.002

Rogowska J, Olkowska E, Ratajczyk W, Wolska L (2018) Gadolinium as a new emerging contaminant of aquatic environments. Environ Toxicol Chem 37:1523–1534. https://doi.org/10.1002/etc.4116

Runge VM (2018) Dechelation (Transmetalation): consequences and safety concerns with the linear Gadolinium-Based contrast agents, in view of recent health care rulings by the EMA (Europe), FDA (United States), and PMDA (Japan). Invest Radiol 53:571. https://doi.org/10.1097/RLI.0000000000000507

Saéz C, Bautista A, Nikolenko O et al (2024) Occurrence and fate of perfluoroalkyl and polyfluoroalkyl substances (PFAS) in an urban aquifer located at the Besòs river Delta (Spain). Environmental Pollution Submitted

Sáez C, Bautista A, Nikolenko O et al (2024) Occurrence and fate of perfluoroalkyl and polyfluoroalkyl substances (PFAS) in an urban aquifer located at the Besòs river Delta (Spain). Environ Pollut 358:124468. https://doi.org/10.1016/j.envpol.2024.124468

Shahhosseini M, Doulati Ardejani F, Baafi E (2017) Geochemistry of rare Earth elements in a neutral mine drainage environment, Anjir tangeh, Northern Iran. Int J Coal Geol 183:120–135. https://doi.org/10.1016/j.coal.2017.10.004

Sherry AD, Caravan P, Lenkinski RE (2009) Primer on gadolinium chemistry. J Magn Reson Imaging 30:1240–1248. https://doi.org/10.1002/jmri.21966

Shiller AM (2002) Seasonality of dissolved rare Earth elements in the lower Mississippi river. Geochem Geophys Geosyst 3:1–14. https://doi.org/10.1029/2002GC000372

Smith C, Liu X-M (2018) Spatial and Temporal distribution of rare Earth elements in the Neuse river, North Carolina. Chem Geol 488:34–43. https://doi.org/10.1016/j.chemgeo.2018.04.003

Sommer K, Sperling M, Karst U (2022) Species-dependent interaction of Gd-based contrast agents with humic substances. Chemosphere 300:134528. https://doi.org/10.1016/j.chemosphere.2022.134528

Song H, Shin W-J, Ryu J-S et al (2017) Anthropogenic rare Earth elements and their Spatial distributions in the Han river, South Korea. Chemosphere 172:155–165. https://doi.org/10.1016/j.chemosphere.2016.12.135

Souza LA, Pedreira RMA, Miró M, Hatje V (2021) Evidence of high bioaccessibility of gadolinium-contrast agents in natural waters after human oral uptake. Sci Total Environ 793:148506. https://doi.org/10.1016/j.scitotenv.2021.148506

Tang J, Johannesson KH (2010) Rare Earth elements adsorption onto Carrizo sand: influence of strong solution complexation. Chem Geol 279:120–133. https://doi.org/10.1016/j.chemgeo.2010.10.011

Trapasso G, Chiesa S, Freitas R, Pereira E (2021) What do we know about the ecotoxicological implications of the rare Earth element gadolinium in aquatic ecosystems? Sci Total Environ 781:146273. https://doi.org/10.1016/j.scitotenv.2021.146273

Vázquez-Suñé E, Carrera J, Tubau I et al (2010) An approach to identify urban groundwater recharge. Hydrol Earth Syst Sci 14:2085–2097. https://doi.org/10.5194/hess-14-2085-2010

Velasco V, Cabello P, Vázquez-Suñé E et al (2012) A sequence stratigraphic based geological model for constraining hydrogeological modeling in the urbanized area of the quaternary Besòs delta (NW mediterranean coast, Spain). 10:373–393. https://doi.org/10.1344/105.000001757

Verplanck PL, Taylor HE, Nordstrom DK, Barber LB (2005) Aqueous stability of gadolinium in surface waters receiving sewage treatment plant effluent, boulder creek, Colorado. Environ Sci Technol 39:6923–6929. https://doi.org/10.1021/es048456u

Wang T, Wu Q, Wang Z et al (2021) Anthropogenic gadolinium accumulation and rare Earth element anomalies of river water from the middle reach of Yangtze river basin, China. ACS Earth Space Chem 5:3130–3139. https://doi.org/10.1021/acsearthspacechem.1c00238

Zhang F, (George), Yeh G-T, Parker JC (eds) (2012) Groundwater reactive transport models. Bentham Science, Oak Park, Illinois, EE. UU

Zhu Z, Liu C-Q, Wang Z-L et al (2016) Rare Earth elements concentrations and speciation in rainwater from guiyang, an acid rain impacted zone of Southwest China. Chem Geol 442:23–34. https://doi.org/10.1016/j.chemgeo.2016.08.038

Zocher A-L, Ciesielski TM, Piarulli S et al (2025) Tracing emerging contaminants from the Baltic sea and North sea in Fjord waters in Southern Norway with rare Earth elements as far-field tracers. Environ Pollut 126124. https://doi.org/10.1016/j.envpol.2025.126124

## Authors and Affiliations

**Estanislao Pujades-Garnes[1] · Mert Çetin Ekiz[2] · Maria Izquierdo[1] · Laura Scheiber[1] · Nafiseh Salehi Siavashani[1] · Anna Jurado[1] · Enric Vázquez-Suñé[1] · Jan Willem Foppen[3]**

✉ Estanislao Pujades-Garnes
estanislao.pujades@idaea.csic.es

[1] Department of Geosciences, Institute of Environmental Assessment and Water Research (IDAEA-CSIC), Jordi Girona 18, Barcelona 08034, Spain

[2] CNR National Research Council, IRSA Water Research Institute, Via Francesco De Blasio 5, Bari 70132, Italy

[3] Water Resource Section, Department of Civil Engineering and Geoscience, Delft University of Technology, Stevinweg 1, Delft 2628 CN, Netherlands